Functional Multiplicity of Motor Molecules Revealed by a Simple Kinetic Analysis

Ellen Lark,‡ Charlotte K. Omoto,‡ and Mark F. Schumaker*
*Department of Pure and Applied Mathematics, and ‡Department of Genetics and Cell Biology, Washington State University, Pullman, Washington 99164-4234 USA

ABSTRACT We present a simple analytical solution for a kinetic model of motor molecule function with multiple arms. This model has a rate of motion proportional to the probability that all arms in a complex are detached from the cytoskeleton and, therefore, we refer to it as obligate cooperativity. The model has the form: $v = V_{max}/(1 + q/S)^n$, where V_{max} is the maximum velocity, the product nq is the effective Michaelis constant at high [ATP], and n is the number of arms. Values of $n = 2$ and $n = 1$ give good fits to the heavy meromyosin and myosin S1 sliding velocity data, respectively, consistent with the number of active sites. Despite the complexity of the eukaryotic axoneme, beat frequency data from Chlamydomonas wild-type and oda mutants are also fit by this model.

INTRODUCTION

Many motor molecules, including myosins, dyneins, and kinesins, have multiple active sites, referred to as arms. The individual arms have been demonstrated to be capable of producing movement in both myosin and dynein (Toyoshima et al., 1987; Moss et al., 1992). To understand the behavior of a multimeric enzyme that interacts with a common cytoskeletal element, we have developed an analytical solution to a 4-state kinetic model of mechanochemical enzymes with multiple active sites, which we call obligate cooperativity (Omoto et al., 1991). This term originates from the observation that the rate of motor molecule movement is proportional to the calculated probability that all of the arms in a complex are detached from the cytoskeleton. We used this model to investigate the ramifications of multiple arms in motor molecule function. Because dissociation of an arm from the cytoskeleton requires the binding of the substrate, MgATP, obligate cooperative interactions are most evident at the lowest substrate concentrations. This substrate dependence contrasts with that of traditional positive cooperativity, in which the cooperative interaction is most evident near the K_M of the enzyme (Cleland, 1970; Segel, 1975).

MATERIALS AND METHODS

Chlamydomonas reinhardtii mutants were kindly provided by the Chlamydomonas Genetics Center, Department of Botany, Duke University, Durham, NC (curator Dr. Elizabeth Harris). Chlamydomonas were bubbled with 5% CO_2 in modified Sager and Granick media (Sager and Granick, 1953) and grown on a 12 h dark/12 h light cycle.

Chlamydomonas reinhardtii was reactivated in a manner similar to Omoto and Brokaw (1985). Cells were concentrated by centrifugation in a table-top centrifuge and washed twice with cold 10 mM HEPES, 5 mM $MgSO_4$, 2 mM EGTA, 1 mM DTT, 0.4% sucrose pH 7.4 (HMDES), and resuspended in 30 mM HEPES, 5 mM $MgSO_4$, 1 mM DTT, 2 mM EGTA, and 25 mM Kacetate pH 7.4 (HMDEK). The cells were stored in this solution on ice until used. To demembranate, the cell suspension was incubated 1:1 with HMDEK + 0.5% NP-40 for 1.5 min in a 15°C waterbath. From here on, all solutions and procedures were done at 15°C to ease the temperature shift from ice to 20°C, at which the experiments were performed. The demembranated cell suspension was mixed 1:9 with reactivation solution which, in addition to HMDEK, contained 2% polyethylene glycol (15,000–20,000 molecular weight), 1 μl/ml (1 mg/ml staurosporine in dimethylsulfoxide) and appropriate [ATP]. Staurosporine (Kamiya Biomedical, Thousand Oaks, CA) was used as a more convenient and potent protein kinase inhibitor than that previously described (Hasegawa et al., 1987). To maintain ATP concentrations below 50 μM, 1 mM phosphoenolpyruvate and 10 units/ml of pyruvate kinase were used for ATP regeneration. The reactivated cells were observed by darkfield microscopy at 20°C. Beat frequency was determined by matching the motion with strobe or at low frequencies by timing the duration of 5–20 beats. Each data point is the mean of 10–20 different flagella except where noted.

Myosin S1 sliding velocity was measured essentially as in Harada et al. (1990), except that the temperature was 28°C, [KCl] was 35 mM, 1.25 mM DTT was used instead of β-mercaptoethanol, and chicken rather than rabbit was the source of S1.

Except for the heavy meromyosin velocity data, kindly provided by Homsher et al. (1992), each data point was calculated by pooling the data from two to four experiments and calculating the mean. The SEM (standard error of the mean) was also calculated for each data point from the pooled data. Outlier data points that deviated by more than 5 SEM from the optimal fit for n (see below) were not used. Points that deviated by 3–5 SEM were eliminated from the analysis unless there appeared to be a systematic deviation between the data and the fit. Such an apparent systematic deviation was encountered only in the analysis of the oda-2 mutant, shown in Fig. 3, *A* and *C* below.

MODEL

A simple 4-state kinetic model of axonemal motion using two arms was previously introduced to model obligate cooperative behavior (Omoto et al., 1991) based on the mechanochemical cycle of actomyosin (Fig. 1 *A*) (Lymn and Taylor, 1971). The two arms were treated as identical and cycling independently. Motivated by the idea that sliding cannot proceed if any arm in a complex remains bound to the cytoskeleton, the proportion of motor molecules with both arms

Received for publication 27 August 1993 and in final form 10 May 1994.
Address reprint requests to Charlotte K. Omoto, Department of Genetics and Cell Biology, Washington State University, Pullman, WA 99164-4234. E-mail: omoto@wsumath.bitnet.

0006-3495/94/09/1134/07 $2.00

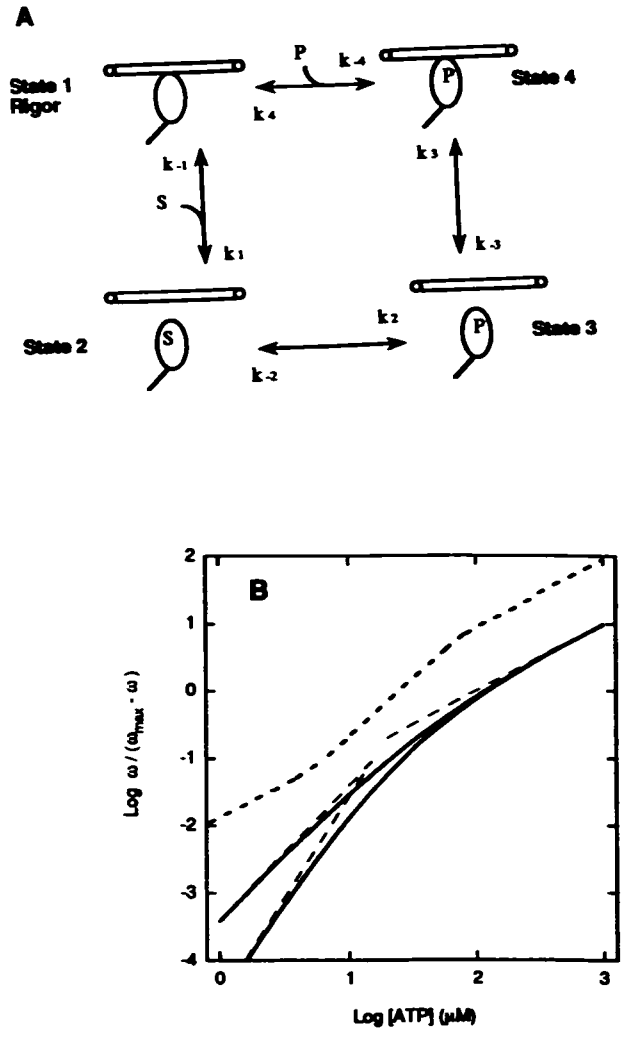

FIGURE 1 (*A*) Four-state mechanochemical cycle for one arm. The rigor state, #1, is released by the binding of the substrate *S*, representing ATP, giving state #2. This is followed by ATP hydrolysis and state #3. The products are represented by P, with no distinction made between ADP and inorganic phosphate. The enzyme-product complex reassociates with cytoskeleton, giving state #4. Reassociation enhances the rate of product release, completing the cycle. (*B*) Hill plots of the obligate cooperativity model, Eq. 2, are given for $n = 2$ and 3 by the solid curves. These curves were constructed using $V_{max} = 50\ s^{-1}$ and $nq = 100\ \mu M$. The asymptotes for the high substrate regime, with a slope of 1, and for the low substrate regime, with slope of *n*, are given by the thin dashed lines (see Eq. 5). The dotted curve sketches a traditional positive cooperative system, showing a maximal Hill coefficient of 1.7 around an ordinate value of 0, corresponding to $S = q$, and slopes decreasing to 1 at both extremes of substrate concentrations. A value of $q = 25\ \mu M$ was used to offset this curve to the left for visual clarity.

detached as a function of substrate concentration was calculated and found to correlate with the experimental observations of sea urchin sperm beat frequency.

We now generalize this model to *n* arms. The cycle is further assumed to be in steady state, and the concentration of products to be negligible. These assumptions are reasonable because the rate remains constant over the course of the experiment.

Consider the state diagram for a single arm, shown in Fig. 1 *A*. S represents the substrate, MgATP, and P represents the products, with no distinction being made between ADP and inorganic phosphate. The forward direction is counterclockwise around the cycle, with rate constants k_i denoting transitions from state *i*. The substrate concentration is assumed to be effectively constant on the time scale of the experiment, and all rate constants are treated as first order. Reverse rate constants are denoted k_{-i}, and the product concentration is assumed to be so low that k_{-4} is set to 0. Standard methods of steady-state enzyme kinetics (King and Altman, 1956; Plowman, 1972) are employed to calculate the probabilities of individual states.

Let P_i be the probability of state *i*, and P_D the probability that an arm is detached from the cytoskeleton. Then P_D is given by

$$P_D = P_2 + P_3 = \frac{(D_2 + D_3)}{(D_1 + D_2 + D_3 + D_4)},$$

where, in the absence of products,

$$D_1 = k_2k_3k_4 + k_{-1}k_3k_4 + k_{-1}k_{-2}k_4 + k_{-1}k_{-2}k_{-3},$$

$$D_2 = k_1k_3k_4 + k_1k_{-2}k_4 + k_{-2}k_{-3}k_1,$$

$$D_3 = k_1k_2k_4 + k_1k_2k_{-3},$$

$$D_4 = k_1k_2k_3,$$

In these equations, the pseudo-first-order rate constant k_1 is proportional to the substrate concentration *S*, which remains constant. We write this as $k_1 = k'_1S$. Then probability P_D has the form

$$P_D = \frac{aS}{bS + c},$$

where *a*, *b*, and *c* are combinations of the rate constants and k'_1. This can be written as

$$P_D = \frac{p}{1 + q/S}, \quad (1)$$

where $P = a/b$ and $q = c/b$.

Assuming that the arms cycle independently, the probability that all *n* arms in a complex are detached is P_D^n. If the observed rate of sliding or beat frequency, v, is proportional to P_D^n, then our model has a very simple analytical solution:

$$v = \frac{V_{max}}{(1 + q/S)^n}, \quad (2)$$

where the maximum rate $V_{max} = FP^n$, with *F* being the constant of proportionality. When the substrate concentration is high, $S \gg q$, we see that $v \approx V_{max}/(1 + nq/S)$. In this regime, nq may be estimated as the effective Michaelis constant.

The formula derived above for obligate cooperativity contrasts with the classical Hill relationship (Hill, 1925)

$$v = \frac{V_{max}}{1 + (q/S)^n}, \quad (3)$$

where v is the reaction velocity, V_{max} is its maximal value, S is the substrate concentration, and q is the value of S giving $v = V_{max}/2$. The exponent n is the Hill coefficient. This formula represents a perfectly cooperative interaction among n subunits. A Hill plot is constructed by plotting $\log v/(V_{max} - v)$ as a function of $\log S$. When Eq. 3 is transformed in this way, a straight line is obtained with slope n

$$\log \frac{v}{V_{max} - v} = n \log S - n \log q. \quad (4)$$

When a Hill plot is constructed for an obligate cooperative interaction, Eq. 2, the following asymptotes are found at high and low substrate concentrations

$$\log \frac{v}{V_{max} - v} = \begin{cases} \log S - \log nq & (S \gg q) \\ n \log S - n \log q & (S \ll q), \end{cases} \quad (5)$$

with a curve interpolating smoothly at intermediate concentrations. The effective Hill coefficient increases from 1 at high S to a limiting value of n at low S. In Fig. 1 *B*, curves are shown for $n = 2$ and 3, with fixed V_{max} and nq. The asymptotes, Eq. 5, are also shown. In contrast, traditional cooperative systems give Hill plots whose highest slope is observed near K_M, that is, near an ordinate value of zero, and is usually less than the number of cooperative units. The slopes of Hill plots of traditional cooperative systems decrease to 1 at both extremes of substrate concentration. Such a curve is sketched schematically in Fig. 1 *B*.

The procedure for determining an optimal fit of the obligate cooperativity model to the data uses the experimental value for V_{max}, which is well determined by the data. Values of nq (the effective K_M) and n are then obtained by two successive optimizations, each involving only one of the variables. We first consider values of n in the interval $0.1 \leq n \leq 5.0$, in steps of $\Delta n = 0.1$. For each value of n, nq is optimized to give the minimal RMS error between the data and the fit, in units of the experimental SEM. That is, in the calculation of the RMS error, the difference between a measured velocity and the model fit was divided by the SEM at each experimental [ATP]. We then choose as optimal the value of n that gives the lowest overall RMS error for both n and nq. Figs. 2 *A* and 3 *A* show the RMS errors as a function of n for the myosin sliding velocity and axonemal beat frequency data, respectively.

Error bars on Hill plots were calculated by propagating uncertainties in both v and V_{max} using the formula

$$\text{error} = \pm \frac{1}{2.3} \left[\frac{V_{max}^2 \Delta v^2 + v^2 \Delta V_{max}^2}{v^2 (V_{max} - v)^2} \right]^{1/2}, \quad (6)$$

where v and V_{max} are mean values for rate measurements; Δv and ΔV_{max} indicate twice the SD of the mean. When v is close to V_{max}, the error bars are very large because of the small denominator in Eq. 6, reflecting the singularity in the ordinate of the Hill plot at $v = V_{max}$. This does not signify a large uncertainty in the experimental values. Such error bars are deleted when they clutter the figure.

RESULTS

Fit of the obligate cooperative model to myosin in vitro sliding velocity data

We searched for in vitro HMM sliding velocity data that covered a wide range of [ATP] with sufficient data points at high [ATP] to provide good estimates for V_{max} and K_M and sufficient data points at very low [ATP] to allow for good fit for the value n. The heavy meromyosin sliding velocity data of Homsher et al. (1992) fit these criteria well (Fig. 2, *B* and *D*). We compared these HMM results with our own myosin S1 sliding velocity data. The myosin S1 sliding velocity data are pooled from two experiments.

The fit of the obligate cooperativity model to the experimental data was examined in several ways. We first determined the optimal value of n by plotting values of n against the RMS error as shown in Fig. 2 *A* for heavy meromyosin and single headed myosin sliding velocities. This plot gives us an indication of how well the model fit the data. The point at which the RMS error is at a minimum for n is the one that we considered optimum. The optimal fit for n for heavy meromyosin is close to two. That for single headed myosin is around one. Thus, this method finds $n = 1$ for the single headed myosin and $n = 2$ for the heavy meromyosin.

An Eadie-Hofstee plot for heavy meromyosin sliding velocity data is shown in Fig. 2 *B*. In the case of true Michaelis-Menten kinetics, the Eadie-Hofstee plot would be a straight line with a negative slope of $-K_M$ and the y-intercept of V_{max}. The high substrate regime corresponds to the data points in the upper left, with decreasing substrate concentration to intermediate levels in the lower right. In the case of heavy meromyosin in vitro sliding, however, the data at lower substrate concentrations curve inward towards the lower left, showing a clear deviation from Michaelis-Menten kinetics.

Sliding velocities calculated using the obligate cooperativity model, Eq. 2, are shown by the curves in Fig. 2, *B* and *D*. In the Eadie-Hofstee plot (Fig. 2 *B*), the abscissa and ordinate both depend on the sliding velocity; therefore, comparisons between fits and the data should be made point-by-point, for each substrate concentration.

The heavy meromyosin data are shown as an Eadie-Hofstee plot in Fig. 2 *B* and as a Hill plot in Fig. 2 *D*. The solid curve was obtained using the maximum sliding velocity, V_{max}, of 5 $\mu m\ s^{-1}$, assuming $n = 2$ and optimizing to find $nq = 62.5\ \mu M$. This curve fits the data well. Because our optimal value for n in Fig. 2 *A* fell between 1 and 2, we also show the fit using $n = 1$ and the effective K_M estimated by Homsher et al. (1992) as a dotted line. The dashed family of curves uses the value for nq optimized for $n = 2$, but shows curves for $n = 1$, 3, and 4. In each case, the curve corresponding to $n = 1$ is a straight line. The curves for $n = 3$ and 4 show large discrepancies from the data at low substrate concentrations. The best fit to the obligate cooperativity model is thus obtained by setting $n = 2$, which is the number of arms per heavy meromyosin.

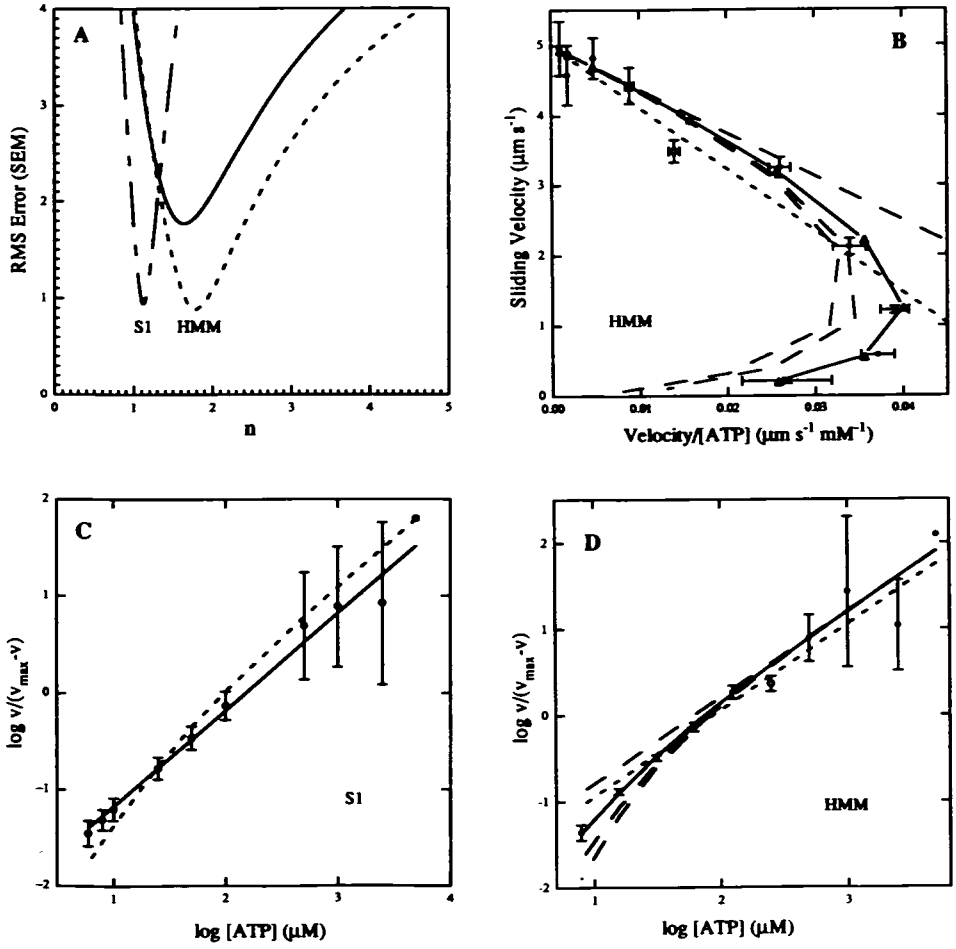

FIGURE 2 Fit of the myosin sliding velocity data to the obligate cooperativity model. Experimental data are shown as circles, with the open circles indicating outliers. Error bars show ± 2 SEMs of the data. Hill plot error bars were constructed using Eq. 6. (*A*) RMS errors plotted for $0.1 \leq n \leq 5.0$ at intervals of $\Delta n = 0.1$. Errors computed for the myosin S1 data are shown by the curve with long and short dashes. No outliers are excluded. The minimum occurs at $n = 1.1$. Errors computed for the heavy meromyosin data with no outliers excluded are shown by the solid curve. The minimum occurs at $n = 1.6$. The dotted curve shows the errors when the single outlier is excluded. The minimum occurs at $n = 1.8$. (*B*) Eadie-Hofstee plot of heavy meromyosin in vitro sliding velocity. All curves were generated by drawing straight line segments between points calculated at each experimental [ATP]. The solid curve, indicated by (Δ), corresponds to $n = 2$ and an optimized nq of 62.5 μM. The dashed curves were constructed using $n = 1$, 3 and 4, and the same nq. The dotted line was constructed using $n = 1$ and $nq = 88.3$ μM, the K_M given by Homsher et al. (1992). The observed $V_{max} = 5.0$ μm s^{-1} was used for all fits. Data were kindly provided by the authors. (*C*) Hill plot of myosin S1 in vitro sliding velocity. The solid line corresponds to $n = 1$ and an optimized nq of 152.4 μM. The dashed line shows the best fit for $n = 2$ with $nq = 80.13$ μM. $V_{max} = 2.069$ μm s^{-1} was used for all fits. Data represent a mean of two experiments. (*D*) Hill plot of heavy meromyosin in vitro sliding velocity. The solid curve shows the best fit for $n = 2$ and an optimized nq of 62.5 μM. The dashed curves were constructed using $n = 1$ to 3, and the same nq. The dotted curves were constructed using $n = 1$ and $nq = 88.3$ μM, the K_M given by Homsher et al. (1992). The observed $V_{max} = 5.0$ μm s^{-1} was used for all fits.

Fig. 2 *C* shows the Hill plot of single-headed myosin. Because the optimum fit to our model falls between 1 and 2 on the RMS error plot (Fig. 2 *A*), we examined the fit using both $n = 1$ (*solid curve*) and $n = 2$ (*dotted curve*), with nq equal to 152.4 and 80.13 μM, respectively. The better fit is shown by $n = 1$, which is the number of arms in single-headed myosin.

Fit of the obligate cooperative model to Chlamydomonas beat frequency data

Wild-type Chlamydomonas axonemes are complex structures containing 24 nm repeats of outer arm dyneins with three heavy chains each and 96 nm repeats of three pairs of inner arm dyneins. We examined the beat frequency of wild-type and two mutants, oda-2 and oda-6, which are totally missing the outer arm dyneins. Fig. 3 *A* shows the RMS errors for optimized fits to the data over a range of values for n at intervals of 0.1. The wild-type data show a very broad minimum for values of n between 3 and 5, reflecting the scatter among the four experimental data sets. Analysis of unpooled wild-type data gives individual minima for three experiments around $n = 3$, but one experiment has a minimum at $n = 6.5$ (data not shown). Thus, the apparent minimum around $n = 4$ is an artifact of the pooled data. The oda-2 data show a minimum RMS error at $n = 2.3$. Only a single data

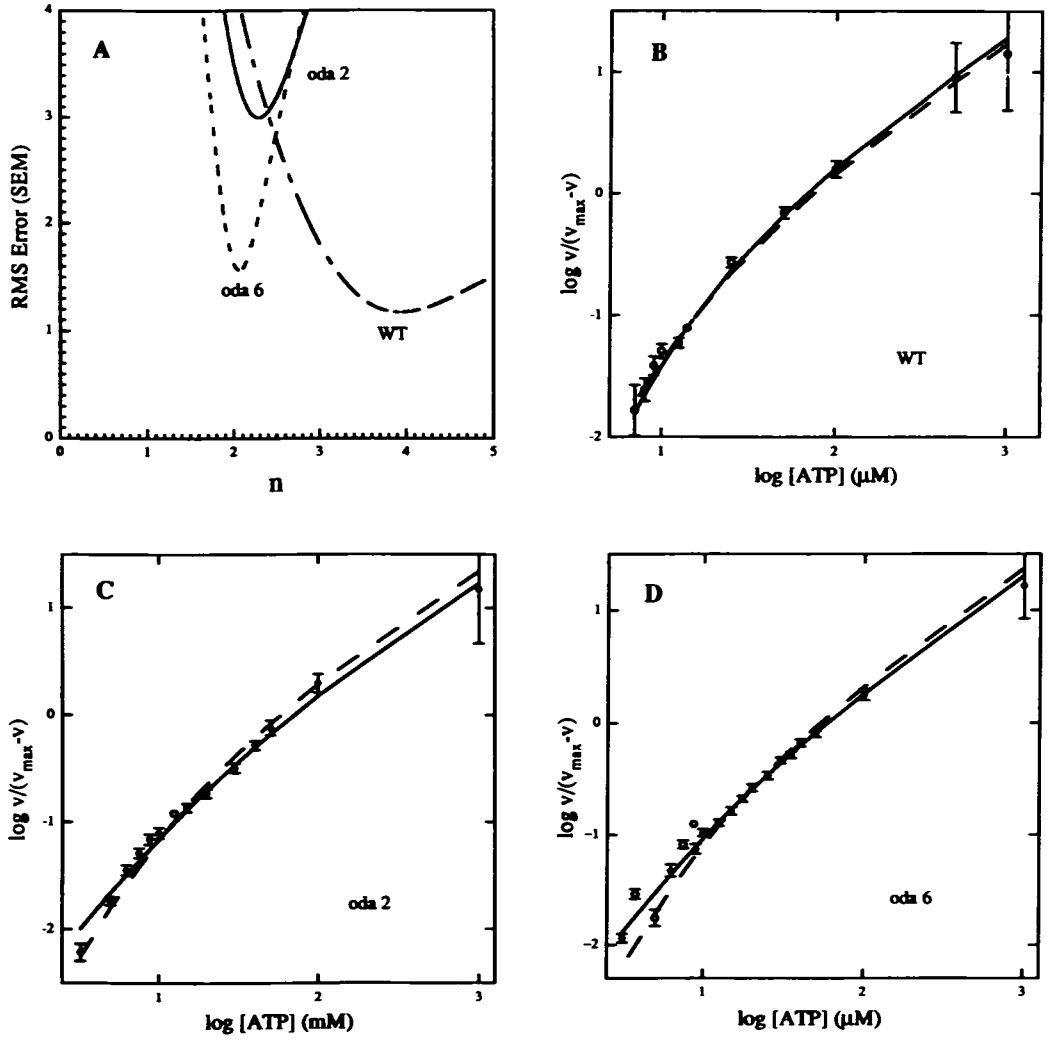

FIGURE 3 Fit of the Chlamydomonas axonemal beat frequency data to the obligate cooperativity model. Data are shown by circles, with the open circles indicating outliers. Error bars show ±2 SEMs of the data. (*A*) RMS errors plotted for $0.1 \leq n \leq 5.0$ at intervals of $\Delta n = 0.1$. Errors computed for the wild-type data are shown by the curve with long and short dashes. The minimum occurs at $n = 3.9$. The fits for oda-2 and oda-6 are shown by the solid and dotted lines; their minima occur at $n = 2.3$ and 2.1, respectively. All errors are computed with outliers excluded. (*B*) Hill plot of wild-type beat frequency. The solid curve was constructed using $V_{max} = 43.5$ hz, with the value $nq = 51.6$ μM determined by optimizing for $n = 4$. The dashed curve gives the best fit for $n = 3$, with the optimized value $nq = 58.1$ μM. Data represent the mean of four experiments. (*C*) Hill plot of oda-2 beat frequency. Curves were constructed using $V_{max} = 26$ hz, $n = 2$ and $nq = 58.8$ μM (——) and $n = 3$ and nq = 45.5 μM (- - - -). The nq values were optimum for the given values of n. Data points represent the mean of two experiments. (*D*) Hill plot of oda-6 beat frequency. Curves were constructed using $V_{max} = 23$ hz, $n = 2$ (——) and $nq = 48.8$ μM; $n = 3$ (- - - -) and $nq = 41.5$ μM. The nq values were optimized as discussed above. Data points represent the mean of three experiments.

point was discarded in the analysis (see Fig. 3 *C*). Further outliers were not eliminated because six data points were found to deviate by 3–5 SEMs from the optimized fit, and this discrepancy appeared to be systematic. The oda-6 data show a minimum RMS error at $n = 2.1$. Four outliers were excluded. These deviated by 6.6 or more SEM from optimized fits to the data.

Fig. 3 *B–D* show Hill plots of the data with various fits to the obligate cooperative model. Two fits of the model to the wild-type data are shown in Fig. 3 *B*, one with $n = 3$ and an optimum nq (effective K_M) of 58.1 μM, and one with $n = 4$ and an optimum nq of 51.6 μM. The two curves appear to fit the data comparably well.

Fig. 3, *C* and *D* show the Hill plots of beat frequency data for Chlamydomonas mutants, which are totally missing the outer arm dyneins, oda-2 and oda-6, respectively. In both cases, two model curves are given using the values of nq derived from best fits with $n = 2$ and $n = 3$, and the estimated value of V_{max}. For oda-2, the optimum fits using $n = 2$ and $n = 3$ are comparably good. However, for oda-6 the fit for $n = 2$ is clearly superior, granting our identification of outliers. For both mutants, the model curves using $n = 2$ fit the data reasonably well. The goodness of fit is reflected in the RMS error for these data in Fig. 3 *A*.

DISCUSSION

The traditional type of positive cooperativity contrasts sharply with our model of obligate cooperativity as diagrammed in Fig. 1 *B*. Qualitatively, the myosin in vitro slid-

ing velocity and axonemal beat frequency data are well described by the obligate cooperative relationship and not at all by either a simple Michaelis-Menten or traditional positive cooperative relationship. The central hypothesis in our obligate cooperative model is that, when a multimeric mechanochemical enzyme interacts with a common cytoskeletal element, the fraction of enzyme species that have all of the arms in a complex detached from the cytoskeleton is directly proportional to the rate of movement. The good fit of this model to two very different types of motor molecule movements strengthens our hypothesis and suggests that the rate of movement is limited by attached motor molecules.

Two key assumptions were necessary to arrive at the simple analytical solution for obligate cooperativity. One assumption is that the arms on motor molecules are equivalent. In the case of heavy meromyosin, the heads of heavy meromyosin are identical. However, there is ample evidence for differences between dyneins in an axoneme, between inner and outer arm dyneins (reviewed in Witman, 1989; Kamiya et al., 1989), and among the outer arm dyneins (Moss et al., 1992; Lark and Omoto, 1994). Another simplifying assumption is that the arms cycle independently. In reality, the rates of cycling of one arm may depend on the state of the other arm. There is kinetic evidence for both myosin and dynein suggesting that when one arm in a complex is attached, the rate of cycling of the other arm increases (Hackney and Clark, 1984; Omoto and Johnson, 1986). The good fit of the model to the data suggests that, for the experimental systems studied here, the effects of arm heterogeneity and nonindependence do not dramatically alter the dynamics of cycling.

The notion of obligate cooperativity was initially introduced to explain the deviation of axonemal beat frequency from simple saturation kinetic behavior. The experimental data analyzed were derived from sea urchin spermatozoa, which have two heavy chains in outer dynein arms (Omoto et al., 1991). It was suggested that the multiplicity of dynein heavy chains in the outer dynein arms was the basis for this cooperative behavior because the slope of the Hill plot (1.45) at the lowest substrate concentration is consistent with two active sites. However, the slope for the data attainable at the lowest substrate concentrations is not a reliable measure of the number of active sites that best fit the obligate cooperative model. In both the model and the data, the slope increases gradually. The model predicts a limiting value of the slope at the lowest substrate concentrations (Fig. 1 *B*, *solid curve*), but it is impossible to know how closely this limit is approached by the experiments. Further, it is technically difficult to measure rates at the lowest substrate concentrations. For these reasons, fitting the model to the entire data set appears to be a more reliable method of estimating the number of active sites. The very simple analytical solution to the model presented in this paper has only three free parameters, which helps to make a fit of the model to data easy to interpret.

Given an ideal data set, both V_{max} and nq (the effective K_M) can be directly determined from the data. For example, in the high substrate regime of the Eadie-Hofstee plot, the y-intercept gives V_{max} and the slope gives $-nq$. Then n could be found by nonlinear curve fitting. The ideal data set would include sufficient data over the highest substrate concentrations to determine accurately V_{max} and nq, and sufficient data over the lowest substrate concentrations to constrain the value for n. However, we have found that this procedure, when applied to actual data, does not yield a very precise value for nq.

Fitting the obligate cooperative model to the data gives a value for n which, in principle, should be an integer representing the functional number of subunits in an oligomeric motor molecule. Our procedure for optimizing n generally yields noninteger values (Figs. 2 *A* and 3 *A*). This may reflect a relatively small number of data points and experimental error, and/or the nonindependence and heterogeneity of the arms.

The best fit of the obligate cooperativity model to the heavy meromyosin sliding velocity data is obtained for $n = 1.8$, close to 2, the number of arms in heavy meromyosin. The model predicts that single-headed myosin data should be fit by $n = 1$. In fact, the in vitro sliding velocity data of myosin S1, a single-headed myosin, are best fit by $n = 1.1$. Thus, this very simple model can interpret in vitro sliding velocities from a well defined system of actin filaments sliding on two- or single-headed myosins.

Eukaryotic axonemes are much more complicated structures with about nine different types of dynein heavy chains. Furthermore, beat frequency is a more complex movement than unloaded in vitro sliding. Thus, it is surprising that the axonemal beat frequency data are fit by this obligate cooperative model as well. Indeed, the value for n is not as well determined by our analysis. For wild-type data, as indicated by the broad minimum in the RMS error plot, the value for n could be 3 or greater. In fact, analysis of individual experiments shows a range of minima from 2.8 to 6.5. This may reflect some inconsistency between experiments. In addition, there may be complex interactions between inner and outer arm dyneins that manifest themselves at different [ATP]. Our experiments were carried out at different ranges of [ATP], and thus might be differentially influenced by these interactions. For mutants totally missing the outer arm dyneins, the optimal value of n appears to be somewhat better defined. A value of $n = 2$ fits both mutant data sets fairly well, consistent with biochemical and electron microscopic observations that suggest that the inner arm dyneins are composed of pairs of heavy chains (Piperno et al., 1990).

The success of this simple obligate cooperative model in quantitatively fitting two very different types of motor molecule function invites analyses of other motor molecule rate data. Further extensions of the model may require inclusion of effects caused by nonidentical active sites and nonindependence in cycling.

We thank Dr. C. J. Brokaw for valuable advice and suggestions. The myosin S1 data could not have been obtained without the help of the members of Dr. T. Yanagida's laboratory. Special thanks are extended to Dr. Harada for teaching C. K. Omoto to do in vitro motility experiments and providing the labeled actin, and to Dr. Tokunaga for providing very pure chicken myosin S1.

This work was supported in part by National Science Foundation grant DCB-8918108 and NSF-CGP Science Fellowship Program to C. K. Omoto.

REFERENCES

Cleland, W. W. 1970. Steady State Kinetics. *In* The Enzymes. Academic Press, New York. 1–65.

Hackney, D. D., and P. K. Clark. 1984. Catalytic consequences of oligomeric organization: kinetic evidence for "tethered" acto-heavy meromyosin at low ATP concentrations. *Proc. Natl. Acad. Sci. USA.* 81: 5345–5349.

Harada, Y., K. Sakurada, T. Aoki, D. D. Thomas, and T. Yanagida. 1990. Mechanochemical coupling in actomyosin energy transduction studied by in vitro movement assay. *J. Mol. Biol.* 216:49–68.

Hasegawa, E., H. Hayashi, S. Asakura, and R. Kamiya. 1987. Stimulation of *in vitro* motility of Chlamydomonas axonemes by inhibition of cAMP-dependent phosphorylation. *Cell Motil. Cytoskel.* 8: 302–322.

Hill, R. 1926. Chemical nature of hemochromogen and its carbon monoxide compound. *Proc. R. Soc. Lond. B.* 100:419–430.

Homsher, E., F. Wang, and J. Sellers. 1992. Factors affecting the movement of F-actin filaments propelled by skeletal muscle heavy meromyosin. *Am. J. Physiol.* 262:C714–C723.

Kamiya, R., E. Kurimoto, H. Sakakibara, and T. Okagaki. 1989. A genetic approach to the function of inner and outer arm dynein. *In* Cell Movement. Alan R. Liss, New York. 209–218.

King, E. L., and C. Altman. 1956. A schematic method of deriving the rate laws for enzyme catalyzed reactions. *J. Phys. Chem.* 60:1375–78.

Lark, E., and C. K. Omoto. 1994. Axonemes paralyzed by the presence of dyneins unable to use ribose-modified ATP. *Cell Motil. Cytoskel.* 27: 161–168.

Lymn, R. W., and E. W. Taylor. 1971. Mechanism of adenosine triphosphate hydrolysis by actomyosin. *Biochemistry.* 10:4617–4624.

Moss, A. G., J.-L. Gatti, and G. B. Witman. 1992. The motile β/IC1 subunit of sea urchin sperm outer arm dynein does not form a rigor bond. *J. Cell Biol.* 118:1177–1188.

Omoto, C. K., and C. J. Brokaw. 1985. Bending patterns of *Chlamydomonas flagella*: II Calcium effects on reactivated *Chlamydomonas flagella*. *Cell Motil. Cytoskel.* 5:53–60.

Omoto, C. K., and K. A. Johnson. 1986. Activation of dynein adenosinetriphosphatase by microtubules. *Biochemistry.* 25:419–426.

Omoto, C. K., J. S. Palmer, and M. E. Moody. 1991. Cooperativity in axonemal motion: analysis of a four-state, two-site kinetic model. *Proc. Natl. Acad. Sci. USA.* 88:5562–5566.

Piperno, G., E. F. Ramanis, E. F. Smith, and W. S. Sale. 1990. Three distinct inner dynein arms in Chlamydomonas flagella: molecular composition and location in the axoneme. *J. Cell Biol.* 110:379–389.

Plowman, K. M. 1972. Enzyme Kinetics. McGraw Hill, New York. 171 pp.

Sager, R., and S. Granick. 1953. Nutritional studies with Chlamydomonas reinhardtii. *Ann. N. Y. Acad. Sci.* 56:831–838.

Segel, I. H. 1975. Enzyme Kinetics. John Wiley & Sons, New York. 346–384.

Toyoshima, Y. Y., S. J. Kron, E. M. McNally, K. R. Niebling, C. Toyoshima, and J. A. Spudich. 1987. Myosin subfragment-1 is sufficient to move actin filaments *in vitro*. *Nature.* 328:536–539.

G. B. Witman. 1989. Composition and molecular organization of the dyneins. *In* Cell Movement. Alan R. Liss, Inc., New York. 25–35.